RESEARCH ARTICLE

Intracellular *Vibrio parahaemolyticus* Escapes the Vacuole and Establishes a Replicative Niche in the Cytosol of Epithelial Cells

Marcela de Souza Santos, Kim Orth

Department of Molecular Biology, University of Texas Southwestern Medical Center, Dallas, Texas, USA

ABSTRACT ***Vibrio parahaemolyticus*** **is a globally disseminated Gram-negative marine bacterium and the leading cause of seafood-borne acute gastroenteritis. Pathogenic bacterial isolates encode two type III secretion systems (T3SS), with the second system (T3SS2) considered the main virulence factor in mammalian hosts. For many decades, *V. parahaemolyticus* has been studied as an exclusively extracellular bacterium. However, the recent characterization of the T3SS2 effector protein VopC has suggested that this pathogen has the ability to invade, survive, and replicate within epithelial cells. Herein, we characterize this intracellular lifestyle in detail. We show that following internalization, *V. parahaemolyticus* is contained in vacuoles that develop into early endosomes, which subsequently mature into late endosomes. *V. parahaemolyticus* then escapes into the cytoplasm prior to vacuolar fusion with lysosomes. Vacuolar acidification is an important trigger for this escape. The cytoplasm serves as the pathogen's primary intracellular replicative niche; cytosolic replication is rapid and robust, with cells often containing over 150 bacteria by the time of cell lysis. These results show how *V. parahaemolyticus* successfully establishes an intracellular lifestyle that could contribute to its survival and dissemination during infection.**

IMPORTANCE **The marine bacterium *V. parahaemolyticus* is the leading cause worldwide of seafood-borne acute gastroenteritis. For decades, the pathogen has been studied exclusively as an extracellular bacterium. However, recent results have revealed the pathogen's ability to invade and replicate within host cells. The present study is the first characterization of the *V. parahaemolyticus*' intracellular lifestyle. Upon internalization, *V. parahaemolyticus* is contained in a vacuole that would in the normal course of events ultimately fuse with a lysosome, degrading the vacuole's contents. The bacterium subverts this pathway, escaping into the cytoplasm prior to lysosomal fusion. Once in the cytoplasm, it replicates prolifically. Our study provides new insights into the strategies used by this globally disseminated pathogen to survive and proliferate within its host.**

Received 19 June 2014 **Accepted** 11 August 2014 **Published** 9 September 2014

Citation de Souza Santos M, Orth K. 2014. Intracellular *Vibrio parahaemolyticus* escapes the vacuole and establishes a replicative niche in the cytosol of epithelial cells. mBio 5(5):e01506-14. doi:10.1128/mBio.01506-14.

Editor Jeff F. Miller, UCLA School of Medicine

Address correspondence to Kim Orth, kim.orth@utsouthwestern.edu.

Vibrio parahaemolyticus is a Gram-negative, halophilic bacterium that naturally inhabits warm marine and estuarine environments (1, 2). Ballast water discharge and rising ocean water temperatures have been associated with *V. parahaemolyticus* dissemination and prevalence worldwide, including southern Alaska (3–5). Recently, this bacterium was identified as the infectious agent responsible for devastating the Southeast Asian shrimp supply, with a consequent global product price increase (6). *V. parahaemolyticus* is recognized as the world's leading cause of acute gastroenteritis through the consumption of contaminated raw or undercooked seafood (7). In immunocompetent individuals, the illness is self-resolving and manifested by diarrhea with abdominal cramps, nausea, vomiting, and low-grade fever (7, 8). However, for individuals with underlying health conditions, infection can cause severe diarrhea and septicemia, the latter correlated with high mortality rates (9). *V. parahaemolyticus* has also been reported to cause infections of seawater-exposed wounds, which in rare cases lead to necrotizing fasciitis and septicemia (10).

Genome sequencing of the pandemic *V. parahaemolyticus* isolate RimD2210633 revealed the presence of two type III secretion systems (T3SS1 and T3SS2), injectisome apparatuses used to directly deliver bacterial proteins (termed effectors) into the host cell (11, 12). T3SS1 is present in all sequenced *V. parahaemolyticus* strains, including both environmental and clinical isolates (13), and is induced by culturing the bacteria in low Ca^{2+}, as with serum-free Dulbecco's modified Eagle's medium (DMEM) tissue culture medium (14). While this system marginally contributes to the bacterium's enterotoxicity (15), the T3SS1 effectors orchestrate a series of events to cause toxicity to cultured cells (16). These events include rapid accumulation of autophagosomes and disruption of cell ion homeostasis, plasma membrane blebbing, cell rounding, and finally lysis (16). T3SS2 was recently acquired through lateral gene transfer (11), and T3SS2 gene clusters are coincident primarily with *V. parahaemolyticus* clinical isolates. In contrast to T3SS1, the expression of T3SS2 genes is induced by bile salts (17). Together, these findings suggest that T3SS2 is important for gastroenteritis. In fact, studies using several mammalian models for *V. parahaemolyticus*-induced enterotoxicity have found T3SS2 to be the key virulence factor responsible for the pathogenic

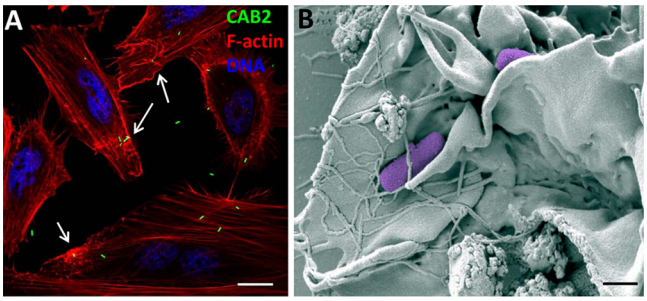

FIG 1 CAB2-induced uptake by epithelial cells. (A) Representative confocal micrograph of HeLa cells infected with CAB2-GFP for 30 min and stained for F-actin and DNA using rhodamine-phalloidin (red) and Hoechst (blue), respectively. White arrows indicate membrane ruffle formation at the site of bacterial entry. Scale bar, 20 μm. (B) Representative electron micrograph of HeLa cells infected with CAB2 for 30 min. Bacteria were pseudocolored in purple. Scale bars, 1 μm.

symptoms associated with gastroenteritis, including diarrhea and intestinal epithelial disruption and inflammation (15, 18, 19).

V. parahaemolyticus has been studied primarily as an extracellular pathogen, subverting host cell functions from the outside through the injection of T3SS effectors. However, the recent characterization of the T3SS2 effector VopC has revealed that *V. parahaemolyticus* can invade host cells. VopC exhibits homology to the catalytic domain of the cytotoxic necrotizing factor (CNF) toxins, which indirectly induce changes in the actin cytoskeleton, facilitating bacterial invasion of host cells through activation of Rho GTPases. Similarly to CNFs, VopC activates Rac1 and CDC42 by deamidating key residues (20). Interestingly, VopC-mediated activation of CDC42 allows bacterial invasion with subsequent intracellular replication within cultured epithelial cells at levels comparable to those of the established intracellular pathogens *Salmonella enterica* serovar Typhimurium (*S.* Typhimurium) and *Shigella flexneri* (20, 21). Despite these interesting findings, the intracellular lifestyle of *V. parahaemolyticus* has not yet been studied.

Intracellular pathogens often invade host cells as a means of escaping extracellular immune defenses. However, internalized pathogens are not entirely protected, as they are normally routed to lysosomes for degradation. Invasive pathogens must devise strategies to avoid this. Typically, intracellular pathogens either (i) reside within a customized, membrane-bound compartment, which limits trafficking along the endosomal pathway, as for *Legionella* and *Brucella* subspp. (22, 23), or (ii) rupture and escape their vacuole to reside and replicate in the host cytosol, as in the case of *Shigella*, *Listeria*, and *Rickettsia* subspp. (22, 24, 25). Recent findings have challenged this canonical classification, as populations of vacuolar and cytosolic pathogens have been observed to escape to the cytosol or reenter endocytic compartments, respectively (25), underscoring the uniqueness of each intracellular pathogen in creating a safe niche for replication within its host.

Given the recent findings supporting the ability of *V. parahaemolyticus* to invade, survive, and replicate within epithelial cells, the goal of the present work was to uncover the strategies used by this pathogen to circumvent lysosomal routing and establish a replicative niche within the host. We found *V. parahaemolyticus*-containing vacuoles have limited interactions with the endosomal pathway, including impaired fusion with lysosomes. Moreover, *V. parahaemolyticus* was revealed to disrupt its vacuole and escape into the cytosol, which became the primary site of replication. Vacuolar acidification was identified as an important factor mediating bacterial vacuolar escape. Through these strategies, *V. parahaemolyticus* successfully establishes an intracellular lifestyle that could contribute to its survival and dissemination during infection.

RESULTS

Invasive *V. parahaemolyticus* induces membrane ruffling of epithelial cells. To study T3SS2-mediated cell invasion independently of other *V. parahaemolyticus* virulence factors, we made use of CAB2, an isogenic strain derived from RimD2210633. The thermostable direct hemolysins (TDH) and the T3SS1 transcriptional

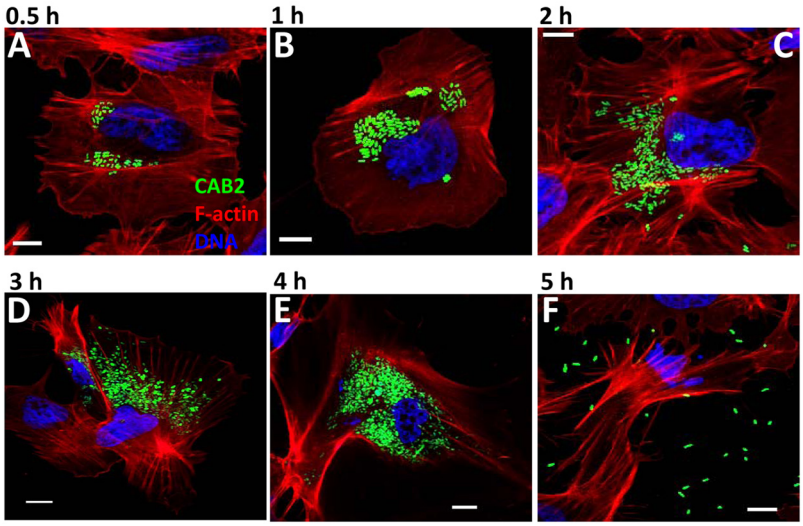

FIG 2 CAB2 intracellular replication. (A to F) Representative confocal micrographs of HeLa cells infected with CAB2-GFP for 75 min and incubated with 100 μg·ml^{-1} gentamicin for the times indicated at the top of each panel. F-actin and DNA were stained using rhodamine-phalloidin (red) and Hoechst (blue), respectively. Scale bars, 10 μm.

regulator gene *exsA* have been deleted in CAB2, but T3SS2 expression is intact (20).

As we previously reported, CAB2 infection of nonphagocytic cells, followed by gentamicin-induced death of extracellular bacteria, revealed an increase in intracellular bacterial numbers over time that precipitously dropped 5 to 6 h after antibiotic incubation (20). In order to visualize bacterial invasion and intracellular replication, HeLa cells were infected with a green fluorescent protein (GFP)-tagged CAB2 strain, and confocal microscopy images were acquired over time.

Following bacterial attachment to the host (30 to 60 min postinfection), we observed membrane ruffling at sites of bacterial entry into HeLa cells stained for actin (Fig. 1A). We also obtained high-resolution scanning electron micrographs of HeLa cells infected with CAB2 for 30 min. Figure 1B shows irregular wave-like membrane folds surrounding entering bacteria. Membrane ruffles induced by *Shigella flexneri* have been described as blossom-like structures near the vicinity of the entering bacterium, composed of parallel microspikes that become interconnected by membrane curtains (26). Membrane ruffle formation induced by *Shigella* is dependent on Rho protein isoforms, which have been shown to not be activated during *V. parahaemolyticus* invasion (20, 21). Instead, epithelial cell invasion by *V. parahaemolyticus* seems to be dependent on activation of CDC42 (21), consistent with the observation that different intracellular pathogens elicit different patterns of membrane folding upon entry (26).

Invasive *V. parahaemolyticus* replicates within and lyses its host cell. Following internalization, we proceeded to visualize intracellular replication of CAB2 using confocal microscopy. As mentioned above, bacterial invasion of HeLa cells was mostly observed between 30 and 60 min postinfection, so we used an infection time of 75 min for all experiments to allow visualization of intracellular bacteria. Following the 75-min infection time, the samples were treated with gentamicin in order to prevent further bacterial internalization. Confocal microscopy images indicated a progressive increase in the intracellular load of CAB2 over time (Fig. 2A to F; see Movie S1 in the supplemental material). We also observed that the invaded HeLa cells were more likely to be found as clusters rather than isolated invaded cells (data not shown). The implications of this observation await further study. Following 4 h of gentamicin treatment, both invaded and noninvaded HeLa cells appeared to shrink; by 5 h, clusters of viable (fluorescent) extracellular CAB2 in the vicinity of round and shrunk HeLa cells were often observed (Fig. 2E and F). The observed pool of viable extracellular bacteria is consistent with host cell lysis prior to cell fixation.

***V. parahaemolyticus* escapes from membrane-bound compartments into the cytosol.** Thus far, we have provided evidence corroborating the view of *V. parahaemolyticus* as an intracellular pathogen (20). Next, we wanted to understand the strategies used by this pathogen to establish and maintain its intracellular life cycle. Following internalization, foreign particles are usually found within membrane-bound compartments that sequentially develop into early and late endosomes for ultimate fusion with lysosomes, where the particles are degraded. We monitored the acquisition of endosomal markers and lysosomal fusion in CAB2-containing vesicles over time using confocal microscopy. Gentamicin was added after bacterial invasion to remove extracellular bacteria, and dual staining of extracellular bacteria was used to differentiate between extracellular and intracellular bacteria. Early after invasion (75 min postinfection), 63.6% ± 10.9% of the intracellular CAB2 was found enclosed within vacuoles that colocalized with early endosomal antigen 1 (EEA1) (Fig. 3A and C), indicating interaction with early endosomes. These interactions were transient, as EEA1 colocalization rapidly decreased to 1.6% ± 1.5% by 1 h post-gentamicin incubation (Fig. 3A and C). As EEA1 colocalization was progressively lost, a relatively constant percentage (around 20%) of intracellular CAB2 was colocalized with late endocytic lysosome-associated membrane protein 1 (lamp-1) (Fig. 3B and C) between 0 and 2 h after gentamicin addition. These findings are consistent with vacuolar maturation. However, lamp-1 acquisition decreased to 2.7% ± 0.4% at 3 h post-antibiotic incubation.

Given the transitory colocalization between CAB2-containing vacuoles and lamp-1, we used transmission electron microscopy (TEM) to assess whether the decrease in lamp-1 retention was due to vacuolar exclusion of lamp-1 or bacterial escape into the cytosol. HeLa cells infected with CAB2 were fixed at 3 h post-gentamicin incubation, a time point at which CAB2 displayed low lamp-1 colocalization (Fig. 3C) and therefore could be highly cytosolic. Under these conditions, the vast majority of CAB2 was found free from membrane-bound compartments (Fig. 3D), consistent with CAB2 localization in the cytoplasm. Further examination of TEM images evidenced several replication events taking place in the cytosol (see Fig. S1 in the supplemental material). We also observed that the number of intravacuolar bacteria clustered in one vacuole was relatively small (1 to 2 bacteria/vacuole on average) and remained constant for the studied time points. Moreover, the majority of the intracellular bacteria were devoid of colocalization with endosomal markers (Fig. 3C). Together, these observations indicate that the cytosol is the primary site of bacterial replication.

Finally, to test whether mature, lamp-1-positive CAB2-containing vacuoles were fused with lysosomes, HeLa cells were initially loaded with Texas Red dextran for 6 h and chased overnight. Under these conditions, dextran is contained mostly within lysosomes. Infection of these cells with CAB2-GFP followed by gentamicin treatment showed no colocalization between dextran and lamp-1-positive CAB2-containing vacuoles from 15 min to 2 h post-antibiotic addition (Fig. 3E). These results suggest that CAB2-containing vacuoles do not fuse with lysosomes and that CAB2 might translocate into the cytosol prior to lysosomal fusion in order to avoid degradation.

Acidification of CAB2-containing vacuoles mediates bacterial escape into the cytosol. Luminal acidification not only is a critical step for progressive maturation of endosomes but has been shown to be essential in triggering vacuolar escape for many intracellular pathogens, including *Listeria monocytogenes* and *Francisella tularensis* (24). To investigate whether vacuolar acidification plays a role in CAB2 escape into the cytoplasm, we first monitored vacuolar acidification over time using the acidification probe LysoTracker Red DND-99, a lysosomotropic agent that concentrates in acidic vesicles and compartments. At 30 min post-gentamicin addition, 24.8% ± 9% of CAB2-containing lamp-1-positive vacuoles acquired the acidic marker (Fig. 4A), although LysoTracker staining was faint for most of the acidified vacuoles. At later time points, such as 1 and 2 h post-antibiotic incubation, about half of the CAB2-containing lamp1-positive vacuoles were colocalized with LysoTracker, and acidification staining was bright (Fig. 4A and B).

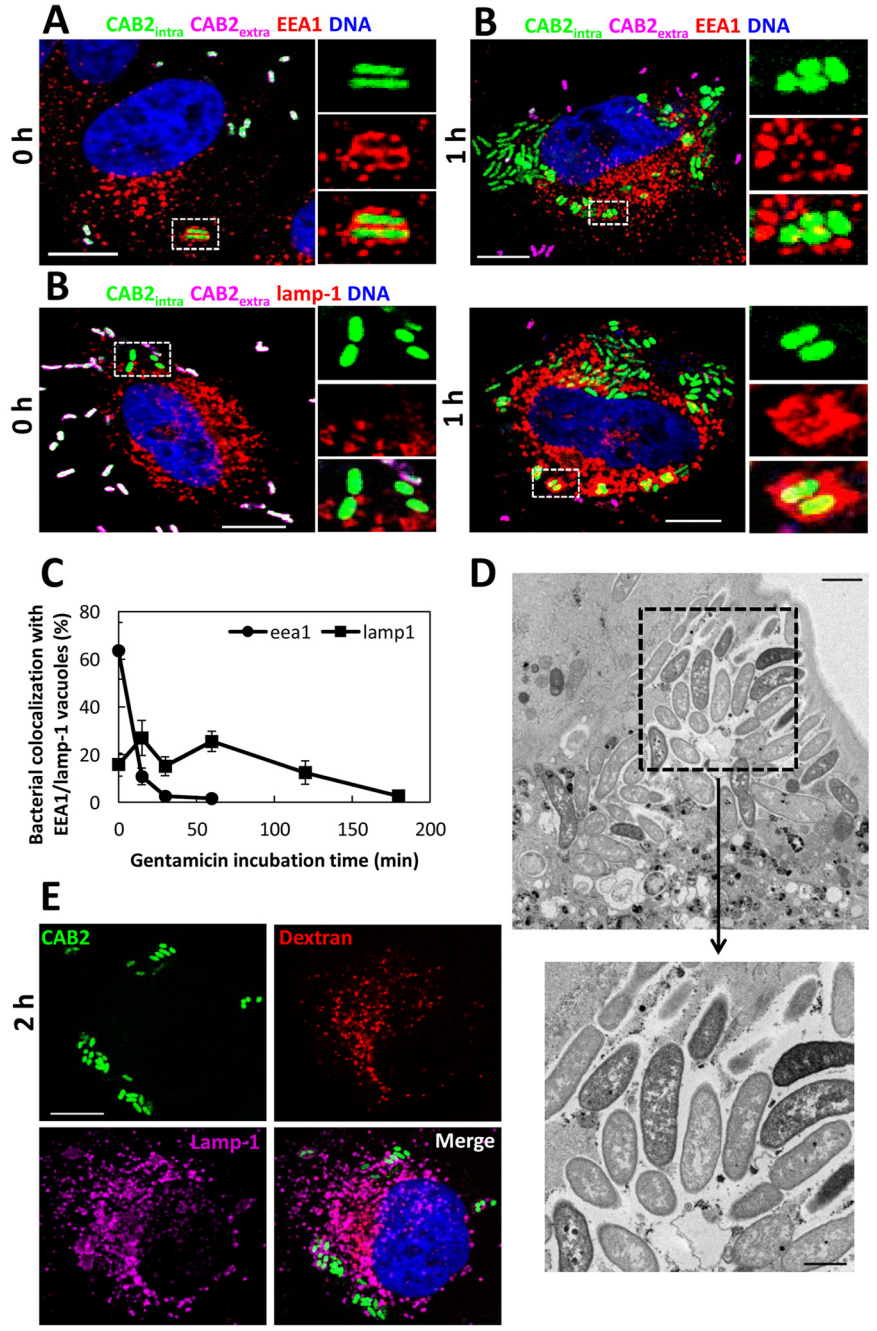

FIG 3 CAB2-containing vacuoles transiently acquire endosomal markers, followed by bacterial escape into the cytosol. (A and B) Representative confocal micrographs of HeLa cells infected with CAB2-GFP for 75 min and incubated with 100 $\mu g \cdot ml^{-1}$ gentamicin for the times indicated on the sides of the panels. Cells were immunostained for EEA1 (A [red]) or lamp-1 (B [red]). Dual staining (green and magenta) was applied to indicate extracellular bacteria, and DNA was stained using Hoechst (blue). White boxes indicate the magnified area to the right of each panel. Scale bars, 10 μm. (C) Enumeration of CAB2-containing vacuoles positive for EEA1 or lamp-1 for the indicated gentamicin incubation times. Over 30 cells were analyzed for each condition. Values are means ± SD ($n = 3$). (D) Representative electron micrograph of HeLa cells infected with CAB2 for 75 min and incubated with gentamicin for 3 h. The boxed region was amplified to highlight the absence of membranes surrounding bacteria. Scale bar in top panel, 1 μm. Scale bar in bottom panel, 10 μm. (E) Representative confocal micrograph of HeLa cells preloaded with 1 $mg \cdot ml^{-1}$ Texas Red dextran (red) for 6 h and chased overnight, after which cells were infected with CAB2-GFP for 75 min and incubated with gentamicin for 2 h. DNA was stained with Hoechst, and late endosomes were immunostained with lamp-1 (magenta).

Having observed acidification of CAB2-containing lamp-1-positive vacuoles, we assessed whether inhibition of vacuolar acidification could affect bacterial escape into the cytosol. Bafilomycin A1 (BAF), a specific inhibitor of the proton vacuolar ATPase (vATPase) pump (27), was used to block acidification of late endosomal compartments and to assess the role of vacuolar acidification for bacterial escape. BAF did not affect bacterial growth in cell culture medium, and BAF inhibited vacuolar acidification at

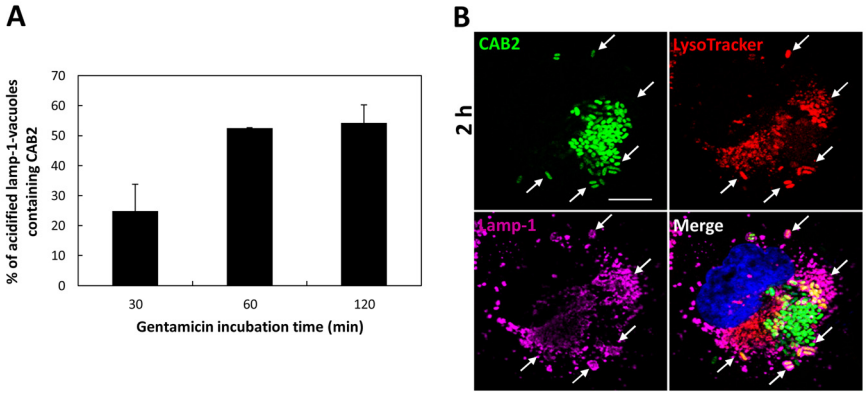

FIG 4 CAB2-containing vacuoles positive for lamp-1 become acidified. (A) Quantification of acidified lamp-1 vacuoles containing CAB2 at the indicated gentamicin incubation times. Values are means ± SD from over 30 cells ($n = 3$). (B) Representative confocal micrograph of HeLa cells infected with CAB2-GFP for 75 min and incubated with 100 μg·ml^{-1} gentamicin for 2 h. During the last 5 min of antibiotic treatment, samples were added with 75 nM Lysotracker Red DND-99 (red). DNA was stained with Hoechst (blue), and late endosomes were immunostained with lamp-1 (magenta). Scale bar, 10 μm.

100 nM (see Fig. S2 and S3 in the supplemental material). Cells were incubated with BAF for 30 min prior to infection, and the drug was kept in the medium throughout both infection and gentamicin treatment. Enumeration of colony-forming units of intracellular CAB2 indicated that BAF treatment significantly reduces intracellular bacterial proliferation (Fig. 5A). Comparison of untreated and BAF-treated samples for bacterial colocalization with lamp-1 using confocal microscopy not only showed a reduction in total intracellular bacterial counts at the single-cell level, corroborating the bulk quantification assay (Fig. 5A), but also revealed a significant retention of CAB2 within lamp-1-positive vacuoles (Fig. 5B and C). As observed in Fig. 5B, vacuolar CAB2

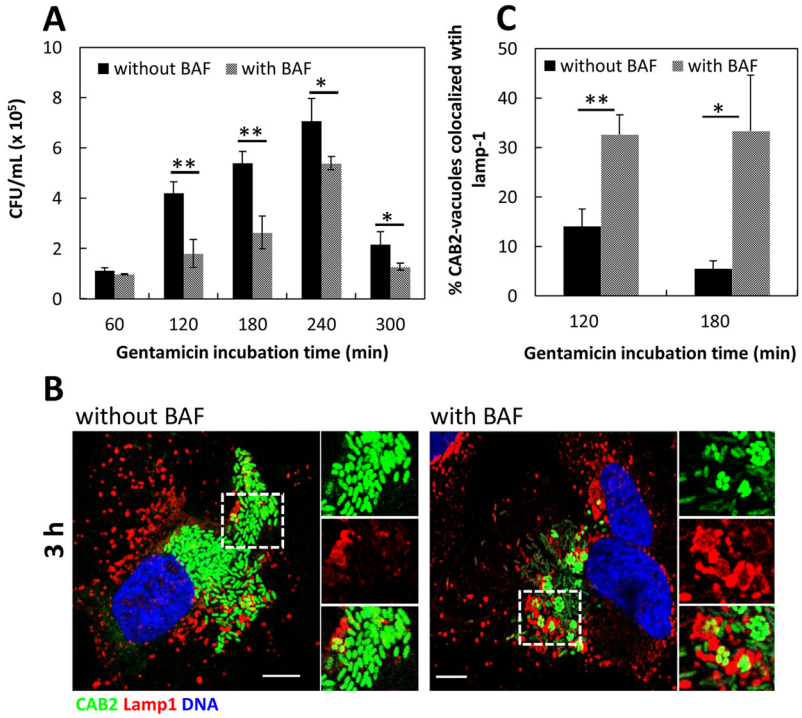

FIG 5 Inhibition of vacuolar acidification impairs bacterial translocation into the cytosol and reduces replication. (A) HeLa cells pretreated or not with 100 nM bafilomycin A1 (BAF) were infected with CAB2 for 75 min and incubated with 100 μg·ml^{-1} gentamicin for the indicated times. Cell lysates were plated and CFU enumerated for intracellular bacteria. Values are means ± SD ($n = 3$). Asterisks indicate statistically significant differences between untreated and BAF-treated samples at 120 ($P = 0.0045$), 180 ($P = 0.0038$), 240 ($P = 0.0372$), and 300 ($P = 0.0420$) min. (B) Representative confocal micrograph of HeLa cells pretreated or not with BAF and infected with CAB2-GFP for 75 min, followed by a 3-h antibiotic incubation. DNA was stained with Hoechst, and late endosomes were immunostained with lamp-1 (red). White boxes indicate the magnified area to the right of each panel. Scale bars, 10 μm. (C) Enumeration of CAB2-containing vacuoles positive for lamp-1 for the indicated gentamicin incubation times, in the absence and presence of BAF. Over 30 cells were analyzed for each condition. Values are means ± SD ($n = 3$). Asterisks indicate statistically significant differences between untreated and BAF-treated samples at 120 ($P = 0.0038$) and 180 ($P = 0.0131$) min.

cells in BAF-treated samples were often brighter than cytosolic bacteria; when we adjusted the fluorescence signal for the vacuolar bacteria, the cytosolic bacteria appeared faint. Confocal analysis of untreated and BAF-treated samples did not suggest apparent differences in the frequency of bacterial cell invasion (data not shown), so it seems unlikely that the reduced intracellular bacterial load resulted from of impaired bacterial uptake. The findings suggest that the intravacuolar pH is an important signal for activation of bacterial factors that mediate vacuolar disruption and escape into the cytosol. Moreover, as BAF treatment resulted in vacuolar retention and decreased replication of CAB2, bacterial escape into the cytosol seems to be crucial for proliferation.

DISCUSSION

V. parahaemolyticus was recently shown to invade, survive, and proliferate within epithelial cells (20). This study is the first description of how *V. parahaemolyticus* turns the intracellular environment into a hospitable niche that allows for efficient bacterial replication. Herein, we provided visual evidence for bacterial uptake by nonphagocytic cells by means of wave-like membrane ruffles and further supported, through both fixed- and live-cell imaging, the capacity of *V. parahaemolyticus* to replicate within its host. Following uptake by HeLa cells, *V. parahaemolyticus*-derived strain CAB2 was found within vacuoles that transiently acquired the early endosome marker EEA1. Progressive CAB2-containing vacuole maturation was indicated by its colocalization with lamp-1. The decrease in lamp-1-positive vacuoles over time, associated with visualization of membrane-free bacteria by TEM, revealed CAB2 to escape its vacuole and take residence in the host cytoplasm, the site for proficient bacterial replication (>150 bacteria/cell). As with other cytosolic bacteria, vacuolar acidification played a role in CAB2 escape into the cytosol, since pharmacological blockage of vacuolar acidification caused a bacterial retention within lamp-1-positive vacuoles and consequent reduction in replication efficiency.

Initially identified as a select group, emerging evidence indicates that many typical vacuolar pathogens can adopt a cytoplasmic phenotype (25). The cytosolic location appears advantageous compared to the luminal vacuole, the former being richer in nutrient supply and devoid of the microbicidal lysosomal components (24). In fact, Knodler et al. demonstrated that a subpopulation of *S.* Typhimurium "hyperreplicates" when in the cytosol, reminiscent of previous findings supporting efficient cytoplasmic replication by an *S.* Typhimurium population defective in maintaining vacuolar integrity (28, 29). Interestingly, the cytosolic "hyperreplicating" subset of *S.* Typhimurium was shown to be invasion primed and to cause epithelial cell death and extrusion for both *in vitro* and *in vivo* models and was responsible for facilitating cell-to-cell spread (28). In addition, Van der Wel et al. reported the cytosolic localization of *Mycobacterium tuberculosis* and *Mycobacterium leprae* to be essential for successful infection, since the avirulent vaccine strain *Mycobacterium bovis* is incapable of vacuolar escape and remains intravacuolar upon invasion of dendritic cells (30).

It has been shown that vacuoles can acidify within 15 min of forming (31), necessitating fast bacterial escape in order for the pathogen to avoid the subsequent lysosomal fusion. Consistent with this, the kinetics of vacuolar escape of many cytosolic pathogens average 15 to 30 min postinvasion (24). As with these pathogens, CAB2 translocates into the cytosol as early as 15 min postgentamicin treatment; this was indicated by the absence of bacterial colocalization with endosomal markers. However, our vacuolar acidification studies indicated that the onset of acidification occurs after the initiation of vacuolar escape (i.e., vacuolar staining with Lysotracker is only detected 30 min after gentamicin treatment). Based on these findings, it is possible that (i) although acidification plays a role for bacterial translocation into the cytosol, pH-independent factors might also contribute to vacuolar escape, and in this case, CAB2 could translocate to the cytoplasm before its vacuole matures into a late endosome and/or acidifies, or (ii) a slight or transient acidification (not detected in our studies using LysoTracker) could be sufficient to trigger bacterial escape early during infection (Fig. 6). In all known cytosolic pathogens, vacuolar disruption relies on secretion of enzymes (24), which many times are only active under acidic pHs, as for listeriolysin O from *Listeria monocytogenes* (32). By identifying the *V. parahaemolyticus* proteins responsible for vacuolar escape—and then assessing whether their activity is dependent on intravacuolar pH—it should be possible to better understand this critical step of the bacterial intracellular life cycle.

The understanding of *V. parahaemolyticus* as an intracellular pathogen is recent. It is thought that the environmental driving force for the evolution of this invasive *V. parahaemolyticus* T3SS2 is a marine animal. Recently, Okada et al., using an infant rabbit model, argued that because invasion is not important for manifestations of acute gastroenteritis (such as intestinal epithelial disruption and fluid accumulation), *V. parahaemolyticus* should be regarded as an extracellular pathogen (21). We suggest that the findings presented here provide strong evidence to the contrary. We propose that the clinical implications of cell invasion by *V. parahaemolyticus* require further consideration, especially with regard to sepsis following both gastroenteritis and necrotizing fasciitis. Importantly, sepsis was not observed in any of the animal models presented to date (15, 18, 19, 33, 34), and the role of cell invasion for the pathogenicity in immunocompromised individuals has not yet been addressed. Interestingly, it has been demonstrated that macrophages derived from chronic granulomatous disease patients infected with the invasive pathogen *Burkholderia cenocepacia* J2315 are more permissive of intracellular replication than normal ones (35). Our studies demonstrate that the bacterium has a complex and deliberate intracellular life cycle: it not only invades but also subverts detrimental trafficking of bacterium-containing vacuoles through the endosomal pathway by means of bacterial translocation from the vacuole to the cytosol, where this pathogen aggressively replicates. Therefore, while the question of the contribution of cell invasion to the disease remains open, it is quite clear from the findings presented here that *V. parahaemolyticus* has acquired the capacity to behave as an intracellular pathogen, and this behavior merits further study.

MATERIALS AND METHODS

Bacterial strains and cell culture. The *V. parahaemolyticus* CAB2 strain was derived from POR1 (RIMD2210633 Δ*tdhAS*), which was generously provided by Tetsuya Iida and Takeshi Honda (18). The CAB2 strain was made by deleting the transcriptional factor ExsA, which regulates T3SS1. CAB2 was grown in Luria-Bertani (LB) medium, supplemented with 3% NaCl, at 30°C. Spectinomycin was added at 50 $\mu g \cdot ml^{-1}$ for growth of CAB2-GFP (15). For induction of T3SS2, overnight CAB2 cultures were subcultured in the presence of 0.05% bile salts for 90 min (17). HeLa cells (ATCC) were maintained in Dulbecco's modified Eagle's medium

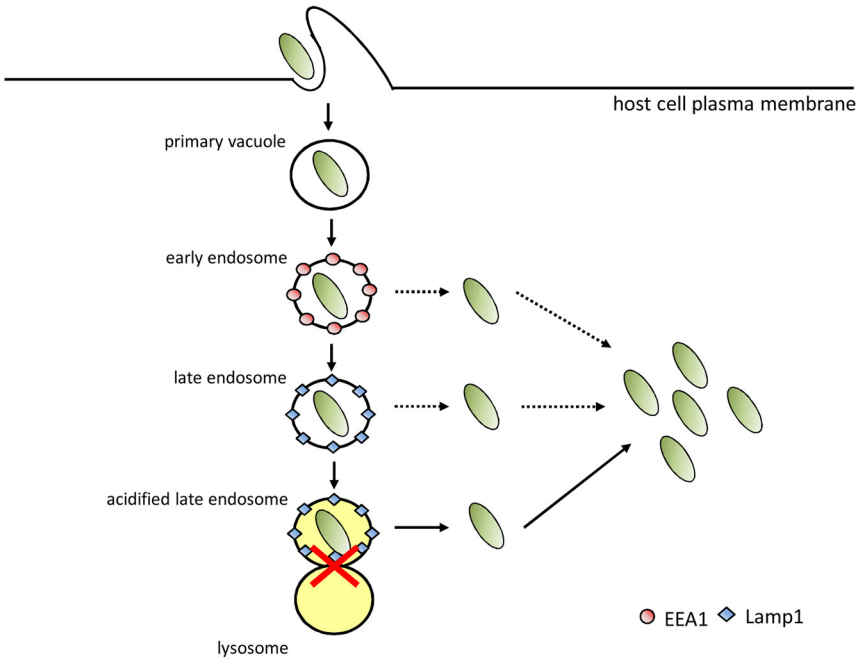

FIG 6 Model for the CAB2 intracellular life cycle. Following invasion, CAB2 is enclosed with a primary vacuole that interacts with early endosomes and acquires EEA1. CAB2-containing vacuoles then traffic to late endosomes, shown by the acquisition of lamp-1, and become acidified. Before detrimental fusion with lysosomes, CAB2 disrupts lamp-1 vacuoles and escapes into the cytosol, where replication takes place. Possible routes of bacterial escape from EEA1- and nonacidified lamp-1-positive vacuoles are indicated by dashed arrows.

(DMEM [Invitrogen]) supplemented with 10% fetal bovine serum and penicillin-streptomycin/glutamine and kept at 5% CO_2.

Antibodies. Rabbit polyclonal anti-*Vibrio parahaemolyticus* O3 and rabbit polyclonal anti-lamp-1 antibodies were obtained from Abcam. Mouse polyclonal anti-EEA1 antibody was purchased from BD Biosciences. Secondary antibodies Alexa Fluor 647/568 goat anti-mouse/rabbit were obtained from Life Technologies, and Alexa Fluor 555 goat anti-mouse from Invitrogen.

Infection protocol. HeLa cells were infected with CAB2 at a multiplicity of infection (MOI) of 10. To synchronize infection, the plates were centrifuged for 5 min at 1000 rpm and then incubated at 37°C in 5% CO_2. For infection times up to 75 min, gentamicin was not applied, but for infection times longer than 75 min, 100 $\mu g \cdot ml^{-1}$ gentamicin was used for the indicated incubation time points in order to kill extracellular bacteria. Where indicated, 100 nM bafilomyicin A1 (LC Laboratories) was added 30 min prior to bacterial infection and kept during the whole infection and gentamicin incubation times.

Labeling of acidified compartments with LysoTracker Red DND-99. For the acidification studies, 75 nM LysoTracker Red DND-99 was added to the samples 5 min prior to cell fixation.

Labeling of lysosomes with Texas Red dextran. HeLa cells were treated with 1 $mg \cdot ml^{-1}$ of Texas Red dextran (Invitrogen) for 6 h and chased overnight. Following lysosome loading with dextran, cell infection proceeded as described above.

Immunofluorescence and confocal microscopy. HeLa cells were seeded onto 6-well plates containing sterile coverslips at a density of 5×10^4 cells/ml. Following infection with CAB2-GFP and gentamicin incubation (when indicated), cells were washed with phosphate-buffered saline (PBS) and then fixed in 3.2% (vol/vol) paraformaldehyde for 10 min at room temperature. Fixed cells were washed in PBS and permeabilized with 0.5% saponin for 4 min at room temperature. After washing with PBS, blocking was performed with 1% bovine serum albumin (BSA) and 0.1% saponin for 30 min at room temperature. Primary and secondary antibodies were diluted in PBS containing 0.5% BSA and 0.1% saponin at appropriate dilutions and incubated serially for 1 h at room temperature. Between each antibody incubation, coverslips were washed three times with PBS containing 0.1% saponin for 5 min each. To differentiate between extra- and intracellular bacteria, coverslips were sequentially incubated with anti-*V. parahaemolyticus* O3 antibody and anti-rabbit Alexa Fluor 647, prior to cell permeabilization. This procedure resulted in double staining for extracellular bacteria only. Nuclei and actin cytoskeleton were stained with Hoechst (Sigma) and rhodamine-phalloidin (Molecular Probes), respectively. Fixed samples were viewed on a Zeiss LSM 710 confocal microscope, and time-lapse microscopy was performed using an Andor spinning-disk confocal microscope. Images and video were converted using ImageJ (NIH).

Scanning electron microscopy. Cells were fixed on coverslips with 2.5% (vol/vol) glutaraldehyde in 0.1 M sodium cacodylate buffer overnight at 4°C. After three washes in 0.1 M sodium cacodylate buffer, cells were postfixed with 1% osmium tetroxide in 0.1 M sodium cacodylate buffer for 45 min. Cells were rinsed with water and dehydrated with increasing concentrations of ethanol, followed by increasing concentrations of hexamethyldisilazane in ethanol. Cells were air dried under the hood, mounted on scanning electron microscopy (SEM) stubs, and sputter coated with gold in a Cressington 108 auto sputter coater. Images were acquired on a field emission scanning electron microscope (Zeiss, Sigma) at 3 kV accelerating voltage.

Transmission electron microscopy. Cells were fixed on MatTek dishes with 2.5% (vol/vol) glutaraldehyde in 0.1 M sodium cacodylate buffer. After three washes in 0.1 M sodium cacodylate buffer, cells were postfixed in 1% osmium tetroxide and 0.8% $K_3[Fe(CN_6)]$ in 0.1 M sodium cacodylate buffer for 1 h at room temperature. Cells were rinsed with water and en bloc stained with 2% aqueous uranyl acetate overnight. After three rinses with water, specimens were dehydrated with increasing concentration of ethanol, infiltrated with Embed-812 resin, and polymerized in a 60°C oven overnight. Blocks were sectioned with a diamond knife (Diatome) on a Leica Ultracut UCT 6 ultramicrotome (Leica Microsystems) and collected onto copper grids, poststained with 2% uranyl

acetate in water and lead citrate. Images were acquired on a Tecnai G^2 spirit transmission electron microscope (FEI) equipped with an LaB_6 source using a voltage of 120 kV.

Gentamicin protection assay. Bacteria were added to triplicate wells of HeLa cell monolayers for infection as described above. At each indicated time point, extracellular bacteria were killed with gentamicin. Monolayers were washed with PBS, and cells were lysed by incubation with LB containing 0.5% Triton X-100 for 10 min at room temperature with agitation. The lysate was serially diluted in LB medium and plated on minimum marine medium (MMM) plates. Plates were incubated at 30°C overnight for subsequent CFU enumeration.

Bacterial growth assay. Triplicates of overnight-grown CAB2 were normalized to optical density at 600 nm (OD_{600}) of 0.1 and grown in DMEM at 37°C with agitation (215 rpm) for 6 h. Growth was assessed by OD_{600} measurements.

Statistical analysis. All data are given as means ± standard deviations (SD) from at least three independent experiments, unless stated otherwise. Statistical analyses were performed by using two-tailed Student's *t* test. A *P* value of <0.05 was considered significant.

SUPPLEMENTAL MATERIAL

Supplemental material for this article may be found at http://mbio.asm.org/lookup/suppl/doi:10.1128/mBio.01506-14/-/DCSupplemental.

Figure S1, PDF file, 0.3 MB.
Figure S2, PDF file, 0.1 MB.
Figure S3, PDF file, 0.1 MB.
Movie S1, AVI file, 0.7 MB.

ACKNOWLEDGMENTS

We thank members of the Orth lab for expert advice and editing.

K.O. and M.S.S. are supported by NIH grant R01-AI056404 and grant I-1561 from the Welch Research Foundation. M.S.S. is supported by NIH grant 5T32DK007745-17. K.O. is a Burroughs Wellcome Investigator in Pathogenesis of Infectious Disease, Beckman Young Investigator, and a W. W. Caruth, Jr., Biomedical Scholar and has an Earl A. Forsythe Chair in Biomedical Science.

REFERENCES

1. **Broberg CA, Calder TJ, Orth K.** 2011. *Vibrio parahaemolyticus* cell biology and pathogenicity determinants. Microbes Infect. **13:**992–1001. http://dx.doi.org/10.1016/j.micinf.2011.06.013.
2. **Zhang L, Orth K.** 2013. Virulence determinants for *Vibrio parahaemolyticus* infection. Curr. Opin. Microbiol. **16:**70–77. http://dx.doi.org/10.1016/j.mib.2013.02.002.
3. **Nair GB, Ramamurthy T, Bhattacharya SK, Dutta B, Takeda Y, Sack DA.** 2007. Global dissemination of *Vibrio parahaemolyticus* serotype O3:K6 and its serovariants. Clin. Microbiol. Rev. **20:**39–48. http://dx.doi.org/10.1128/CMR.00025-06.
4. **Velazquez-Roman J, León-Sicairos N, de Jesus Hernández-Díaz L, Canizalez-Roman A.** 2014. Pandemic *Vibrio parahaemolyticus* O3:K6 on the American continent. Front. Cell. Infect. Microbiol. **3:**110. http://dx.doi.org/10.3389/fcimb.2013.00110.
5. **McLaughlin JB, DePaola A, Bopp CA, Martinek KA, Napolilli NP, Allison CG, Murray SL, Thompson EC, Bird MM, Middaugh JP.** 2005. Outbreak of *Vibrio parahaemolyticus* gastroenteritis associated with Alaskan oysters. N. Engl. J. Med. **353:**1463–1470. http://dx.doi.org/10.1056/NEJMoa051594.
6. **Tran L, Nunan L, Redman RM, Mohney LL, Pantoja CR, Fitzsimmons K, Lightner DV.** 2013. Determination of the infectious nature of the agent of acute hepatopancreatic necrosis syndrome affecting penaeid shrimp. Dis. Aquat. Organ. **23:**128–136. http://dx.doi.org/10.3354/dao02621.
7. **O'Boyle N, Boyd A.** 2014. Manipulation of intestinal epithelial cell function by the cell contact-dependent type III secretion systems of *Vibrio parahaemolyticus*. Front. Cell. Infect. Microbiol. **3:**114. http://dx.doi.org/10.3389/fcimb.2013.00114.
8. **Ham H, Orth K.** 2012. The role of type III secretion system 2 in *Vibrio parahaemolyticus* pathogenicity. J. Microbiol. **50:**719–725. http://dx.doi.org/10.1007/s12275-012-2550-2.
9. **Daniels A, MacKinnon L, Bishop R, Altekruse S, Hammond RM, Thompson S, Wilson S, Bean NH, Griffin PM, Slutsker L.** 2000. *Vibrio parahaemolyticus* infections in the United States, 1973-1998. J. Infect. Dis. **181:**1661–1666. http://dx.doi.org/10.1086/315459.
10. **Tena D, Arias M, Alvarez BT, Mauleón C, Jiménez MP, Bisquert J.** 2010. Fulminant necrotizing fasciitis due to *Vibrio parahaemolyticus*. J. Med. Microbiol. **59:**235–238. http://dx.doi.org/10.1099/jmm.0.014654-0.
11. **Makino K, Oshima K, Kurokawa K, Yokoyama K, Uda T, Tagomori K, Iijima Y, Najima M, Nakano M, Yamashita A, Kubota Y, Kimura S, Yasunaga T, Honda T, Shinagawa H, Hattori M, Iida T.** 2003. Genome sequence of *Vibrio parahaemolyticus*: a pathogenic mechanism distinct from that of *V. cholerae*. Lancet **361:**743–749. http://dx.doi.org/10.1016/S0140-6736(03)12659-1.
12. **Burkinshaw BJ, Strynadka NC.** 2014. Assembly and structure of the T3SS. Biochim. Biophys. Acta **1843:**1649–1669. http://dx.doi.org/10.1016/j.bbamcr.2014.01.035.
13. **Okada N, Matsuda S, Matsuyama J, Park KS, de los Reyes C, Kogure K, Honda T, Iida T.** 2010. Presence of genes for type III secretion system 2 in *Vibrio mimicus* strains. BMC Microbiol. **10:**302. http://dx.doi.org/10.1186/1471-2180-10-302.
14. **Ono T, Park KS, Ueta M, Iida T, Honda T.** 2006. Identification of proteins secreted via *Vibrio parahaemolyticus* type III secretion system 1. Infect. Immun. **74:**1032–1042. http://dx.doi.org/10.1128/IAI.74.2.1032-1042.2006.
15. **Ritchie JM, Rui H, Zhou X, Iida T, Kodoma T, Ito S, Davis BM, Bronson RT, Waldor MK.** 2012. Inflammation and disintegration of intestinal villi in an experimental model for *Vibrio parahaemolyticus*-induced diarrhea. PLoS Pathog. **8:**e1002593. http://dx.doi.org/10.1371/journal.ppat.1002593.
16. **Burdette DL, Yarbrough ML, Orvedahl A, Gilpin CJ, Orth K.** 2008. *Vibrio parahaemolyticus* orchestrates a multifaceted host cell infection by induction of autophagy, cell rounding, and then cell lysis. Proc. Natl. Acad. Sci. U. S. A. **105:**12497–12502. http://dx.doi.org/10.1073/pnas.0802773105.
17. **Gotoh K, Kodama T, Hiyoshi H, Izutsu K, Park KS, Dryselius R, Akeda Y, Honda T, Iida T.** 2010. Bile acid-induced virulence gene expression of *Vibrio parahaemolyticus* reveals a novel therapeutic potential for bile acid sequestrants. PLoS One **5:**e13365. http://dx.doi.org/10.1371/journal.pone.0013365.
18. **Park KS, Ono T, Rokuda M, Jang MH, Okada K, Iida T, Honda T.** 2004. Functional characterization of two type III secretion systems of *Vibrio parahaemolyticus*. Infect. Immun. **72:**6659–6665. http://dx.doi.org/10.1128/IAI.72.11.6659-6665.2004.
19. **Hiyoshi H, Kodama T, Iida T, Honda T.** 2010. Contribution of *Vibrio parahaemolyticus* virulence factors to cytotoxicity, enterotoxicity, and lethality in mice. Infect. Immun. **78:**1772–1780. http://dx.doi.org/10.1128/IAI.01051-09.
20. **Zhang L, Krachler AM, Broberg CA, Li Y, Mirzaei H, Gilpin CJ, Orth K.** 2012. Type III effector VopC mediates invasion for *Vibrio* species. Cell Rep. **1:**453–460. http://dx.doi.org/10.1016/j.celrep.2012.04.004.
21. **Okada R, Zhou X, Hiyoshi H, Matsuda S, Chen X, Akeda Y, Kashimoto T, Davis BM, Iida T, Waldor MK, Kodama T.** 2014. The *Vibrio parahaemolyticus* effector VopC mediates Cdc42-dependent invasion of cultured cells but is not required for pathogenicity in an animal model of infection. Cell. Microbiol. **16:**938–947. http://dx.doi.org/10.1111/cmi.12252.
22. **Méresse S, Steele-Mortimer O, Moreno E, Desjardins M, Finlay B, Gorvel JP.** 1999. Controlling the maturation of pathogen-containing vacuoles: a matter of life and death. Nat. Cell Biol. **1:**E183–E188. http://dx.doi.org/10.1038/15620.
23. **Roy CR, Salcedo SP, Gorvel JP.** 2006. Pathogen-endoplasmic-reticulum interactions: in through the out door. Nat. Rev. Immunol. **6:**136–147. http://dx.doi.org/10.1038/nri1775.
24. **Ray K, Marteyn B, Sansonetti PJ, Tang CM.** 2009. Life on the inside: the intracellular lifestyle of cytosolic bacteria. Nat. Rev. Microbiol. **7:**333–340. http://dx.doi.org/10.1038/nrmicro2112.
25. **Fredlund J, Enninga J.** 2014. Cytoplasmic access by intracellular bacterial pathogens. Trends Microbiol. **22:**128–137. http://dx.doi.org/10.1016/j.tim.2014.01.003.
26. **Adam T, Arpin M, Prévost MC, Gounon P, Sansonetti PJ.** 1995. Cytoskeletal rearrangements and the functional role of T-plastin during entry of *Shigella flexneri* into HeLa cells. J. Cell Biol. **129:**367–381. http://dx.doi.org/10.1083/jcb.129.2.367.

27. **Bowman EJ, Siebers A, Altendorf K.** 1988. Bafilomycins: a class of inhibitors of membrane ATPases from microorganisms, animal cells, and plant cells. Proc. Natl. Acad. Sci. U. S. A. **85:**7972–7976. http://dx.doi.org/10.1073/pnas.85.21.7972.
28. **Knodler LA, Vallance BA, Celli J, Winfree S, Hansen B, Montero M, Steele-Mortimer O.** 2010. Dissemination of invasive *Salmonella* via bacterial-induced extrusion of mucosal epithelia. Proc. Natl. Acad. Sci. U. S. A. **107:**17733–17738. http://dx.doi.org/10.1073/pnas.1006098107.
29. **Brumell JH, Tang P, Zaharik ML, Finlay BB.** 2002. Disruption of the *Salmonella*-containing vacuole leads to increased replication of *Salmonella enterica* serovar Typhimurium in the cytosol of epithelial cells. Infect. Immun. **70:**3264–3270. http://dx.doi.org/10.1128/IAI.70.6.3264-3270.2002.
30. **van der Wel N, Hava D, Houben D, Fluitsma D, van Zon M, Pierson J, Brenner M, Peters PJ.** 2007. *M. tuberculosis* and *M. leprae* translocate from the phagolysosome to the cytosol in myeloid cells. Cell **129:**1287–1298. http://dx.doi.org/10.1016/j.cell.2007.05.059.
31. **Yates RM, Hermetter A, Russell DG.** 2005. The kinetics of phagosome maturation as a function of phagosome/lysosome fusion and acquisition of hydrolytic activity. Traffic **6:**413–420. http://dx.doi.org/10.1111/j.1600-0854.2005.00284.x.
32. **Beauregard KE, Lee KD, Collier RJ, Swanson JA.** 1997. pH-dependent perforation of macrophage phagosomes by listeriolysin O from *Listeria monocytogenes*. J. Exp. Med. **186:**1159–1163. http://dx.doi.org/10.1084/jem.186.7.1159.
33. **Piñeyro P, Zhou X, Orfe LH, Friel PJ, Lahmers K, Call DR.** 2010. Development of two animal models to study the function of *Vibrio parahaemolyticus* type III secretion systems. Infect. Immun. **78:**4551–4559. http://dx.doi.org/10.1128/IAI.00461-10.
34. **Whitaker WB, Parent MA, Boyd A, Richards GP, Boyd EF.** 2012. The *Vibrio parahaemolyticus* ToxRS regulator is required for stress tolerance and colonization in a novel orogastric streptomycin-induced adult murine model. Infect. Immun. **80:**1834–1845. http://dx.doi.org/10.1128/IAI.06284-11.
35. **Al-Khodor S, Marshall-Batty K, Nair V, Ding L, Greenberg DE, Fraser ID.** 2014. *Burkholderia cenocepacia* J2315 escapes to the cytosol and actively subverts autophagy in human macrophages. Cell. Microbiol. **16:**378–395. http://dx.doi.org/10.1111/cmi.12223.